batteries

MDPI

Article

Optimising the Selective Leaching and Recovery of Cobalt, Lanthanum, and Strontium for Recycling End-of-Life Solid Oxide Cells

Martina Bruno [1], Sofia Saffirio [2], Federico Smeacetto [2], Sonia Fiorilli [2] and Silvia Fiore [1,*]

[1] Department of Environment, Land, and Infrastructure Engineering (DIATI), Politecnico di Torino, Corso Duca Degli Abruzzi 24, 10129 Turin, Italy; martina.bruno@polito.it
[2] Department of Applied Science and Technology (DISAT), Politecnico di Torino, Corso Duca Degli Abruzzi 24, 10129 Turin, Italy; sofia.saffirio@polito.it (S.S.); federico.smeacetto@polito.it (F.S.); sonia.fiorilli@polito.it (S.F.)
* Correspondence: silvia.fiore@polito.it

Abstract: This study explored the selective recovery of Co, La, and Sr from end-of-life solid oxide cells (SOCs) using ultrasound-assisted leaching in HCl. HCl concentration (1, 5, and 10 M) and solid-to-liquid ratio (S/L, 100 and 200 g/L) were varied to optimize the efficiency and the selectivity of Co, La, and Sr leaching. Then, they were recovered as oxalates at pH 0.7, 1, and 4. Using 10 M HCl and an S/L ratio of 100 g/L on ball-milled samples achieved 96–99% leaching efficiency but led to Ni impurities from the underneath layers. Thermal pre-treatment at 800 °C decreased Ni leaching by 90% but decreased target metals' recovery by 9%. Direct leaching (without pre-treatments) with 1 M HCl and an S/L ratio of 200 g/L achieved up to 91% leaching efficiency, recovering 42% of Co, 93% of La, and 33% of Sr with minimal Ni impurities. A preliminary economic analysis indicated that avoiding pre-treatments can cut expenses by 96%. An economic analysis indicated that direct leaching is the most cost effective, reducing expenses by up to 96% compared to thermal pre-treatment and high HCl concentrations. This study highlights the potential for an efficient and cost-effective method for recycling Co, La, and Sr from EoL SOCs.

Keywords: end of life; hydrometallurgy; leaching; recycling; solid oxide cell

Academic Editors: Elza Bontempi and Chiara Ferrara

Received: 2 March 2025
Revised: 23 March 2025
Accepted: 24 March 2025
Published: 25 March 2025

Citation: Bruno, M.; Saffirio, S.; Smeacetto, F.; Fiorilli, S.; Fiore, S. Optimising the Selective Leaching and Recovery of Cobalt, Lanthanum, and Strontium for Recycling End-of-Life Solid Oxide Cells. *Batteries* **2025**, *11*, 124. https://doi.org/10.3390/batteries11040124

1. Introduction

Solid oxide cells (SOCs) are highly efficient electrochemical devices that convert chemical energy in gaseous fuels directly into electrical energy [1,2]. SOCs contribute to reducing greenhouse gas (GHG) emissions and provide high electrical efficiency [3,4], making them an ideal technology for transitioning from fossil fuels to renewable energy sources [5]. The fundamental components of SOC systems are an anode, a cathode, and a solid electrolyte [6]. Anodes are made of porous composite ceramic materials conducting oxygen ions and electrons as Ni-YSZ, where Yttria-stabilized Zirconia (YSZ) provides physical, chemical, electrical, and mechanical stability [7–9] and Ni offers high electrical conductivity and catalytic efficiency [10]. Cathodes are mostly based on strontium-doped lanthanum-cobalt oxides (LSC), offering high electrical and ionic conductivity [11,12]. Co, La, and Sr are critical raw materials [13], thereby their recovery and recycling are fundamental to secure the supply chains of strategic sectors and mitigate the environmental impacts associated with mining activities [14–16]. SOCs are relatively less prevalent than other fuel cell technologies, such as proton exchange membrane fuel cells, and dedicated recycling strategies for end-of-life (EoL) SOCs are still underdeveloped [17]. The few

available studies focused on the recovery of Ni and YSZ from anode components, as they constitute most of the SOC mass balance [18,19]; direct recycling of the YSZ layer was also recently proposed by reprocessing of the ceramic components into recycled sintered substrate [20]. A multistep process was recently reported involving in-sequence ball milling (6 h) and hydrothermal treatment (at 200 °C for 4 h) to promote the effective disintegration and pulverisation of the sintered Ni-YSZ composite, followed by 2 M HNO_3 leaching at 80 °C for 2 h, enabling the quantitative recovery of Ni while preserving the YSZ crystalline structure [21]. Another study applied ball milling in ethanol for 5 h followed by 65 %wt. HNO_3 leaching at room temperature, achieving recovery efficiency > 90% for Ni and YSZ [20,22]. Both studies involved a pre-removal of the LSC layer from the EoL SOC by mechanical scratching before the application of the proposed process [21,22]. More recently, ultrasonic de-coating was recommended as a potentially automatable process to separate the LSC layer from the SOC [23]. The primary drawback of these recycling processes, despite the high recovery efficiency achieved for anodic materials, is that the mechanical detachment of the LSC layer entails high energy demand. This results in significant associated costs and GHG emissions [24]. Indeed, a key challenge in SOC recycling is contamination from use, which impacts the quality of recovered materials, requiring the development of cost-effective separation methods to ensure economic feasibility of recycling processes [18].

To the best of our knowledge, the recovery of La, Co, and Sr from EoL SOCs without preventively detaching the LSC layer has not been considered yet. Therefore, this study aimed at optimising a novel and efficient route to recover Co, La, and Sr by exploiting ultrasonic-assisted HCl leaching on EoL SOCs at room temperature without prior detaching of the LSC layer. Compared with previous studies, which required manual or mechanical detachment of the LSC layer [21,25], often affecting the overall economic profit of the recycling process, this work proposes a novel solution to selectively recover Co, La, and Sr while preserving the YSZ layer [20]. The literature reports 12 M HCl leaching efficiency towards Co and La at room temperature [26,27] and YSZ preservation [28]. In this study, operative parameters, such as HCl concentration (1, 5, and 10 M) and solid-to-liquid ratio (S/L, 100 and 200 g/L), were varied to optimize La, Co, and Sr leaching efficiency and selectivity. In addition, selective leaching operations were conducted by following three different pathways (Figure 1): (i) EoL SOCs as dismantled from exhausted stacks were manually fragmented and ball milled before applying HCl leaching (1 and 10 M) in an ultrasound bath at room temperature; (ii) the same procedure as reported in (i) with an additional thermal treatment at 800 °C of milled samples to investigate the effect on leaching efficiency; (iii) ultrasound-assisted HCl leaching applied directly to the EoL SOC samples, without scratching, ball milling, or thermal pre-treatment, adopting an S/L equal to 200 g/L and varying HCl concentration (1 and 5 M). Then, Co, La, and Sr were selectively recovered from the leachate by chemical precipitation as oxalates at different pH values. Finally, a preliminary economic analysis compared the operative costs (energy demand and reagents) of the investigated processes.

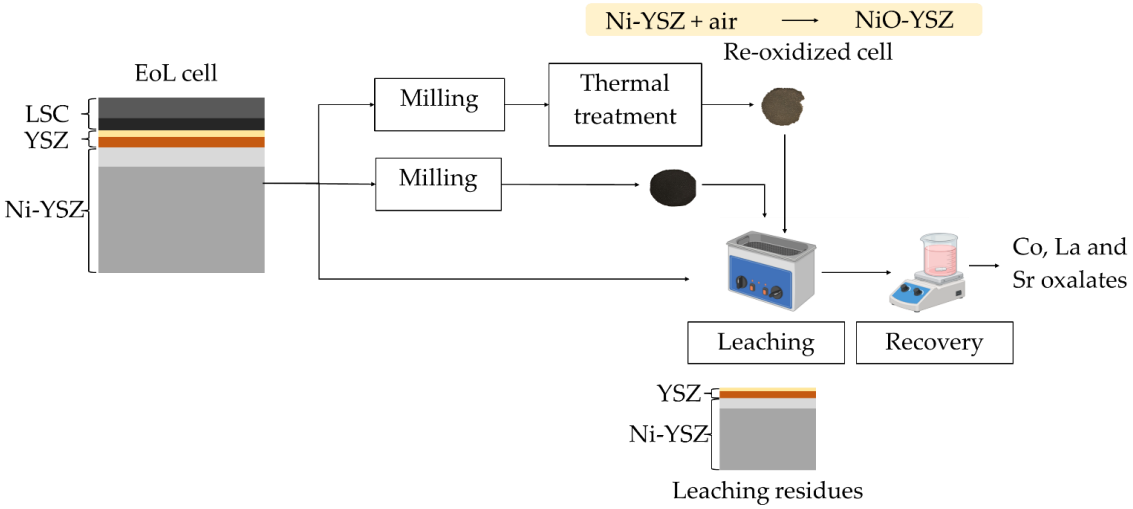

Figure 1. Concept of the study.

2. Materials and Methods

2.1. Samples' Preparation and Characterization

The samples considered in this study were EoL SOCs provided by Elcogen (Elcogen AS, Tallin, Estonia) after stacks' dismantling. The cells were ball milled for 5 min in a Retsch MM200 ball mill with 50 mL zirconia jars and two 10 mm beads in each jar. Before characterization, the milled samples were rinsed with deionized water and dried at 60 °C overnight in an ARGO LAB TCN 30 oven. The milled samples were characterized through X-ray fluorescence (XRF) spectroscopy (Rigaku, NEX-DE), X-ray diffraction (XRD) spectroscopy (PANanalytical X'Pert), scanning electronic microscopy (SEM) equipped with energy-dispersive spectroscopy (EDS) detector (Phenom XL, Alphatest), and inductively coupled plasma atomic emission spectrometry (ICP-AES, Thermoscientific, Waltham, MA, USA, ICAP Q) after digestion in aqua regia. XRF spectroscopy was used to analyse Al, Ca, Ce, Cl, Co, Cr, Cu, Fe, Gd, La, Ni, P, Si, Sr, Ti, V, Y, and Zr, and ICP-AES was used to analyse Ce, Co, Gd, La, Ni, Sr, and Y.

2.2. Ultrasound-Assisted Selective Leaching

Ultrasound leaching of La, Co, and Sr from the ball-milled samples employed HCl at room temperature (20 °C) for 10 min, varying HCl concentration (1 and 10 M) and 100 g/L solid-to-liquid ratio (S/L). The effect of thermal pre-treatment at 800 °C for 60 min (Figure 2) in a ZE V220 Prederi furnace was also explored. The reagents used were hydrochloric acid (37% vol. Carlo Erba Reagents CAS:7647-01-0), sodium hydroxide (≥98% Honeywell/Fluka CAS:1310-73-2), and oxalic acid (≥99% Sigma-Aldrich CAS:6153-56-6).

Each leaching experiment was performed in triplicate on 10 g of ball milled SOC samples. Leaching tests were executed in a Bandelin SONOREX DIGIPLUS DL 514 BH ultrasonic bath (720 W ultrasonic peak power, 180 W ultrasonic nominal power, 35 kHz ultrasound frequency), setting the ultrasound power to 100% in all leaching tests. Ultrasound leaching tests were performed also directly on EoL SOC samples, without manual removal of LSC layer, ball milling, and thermal pre-treatment. The SOC samples were partially immersed for 10 min in HCl (1 M and 5 M) applying 200 g/L S/L, with the LSC cathode side facing downwards. The direct leaching tests were performed in triplicate.

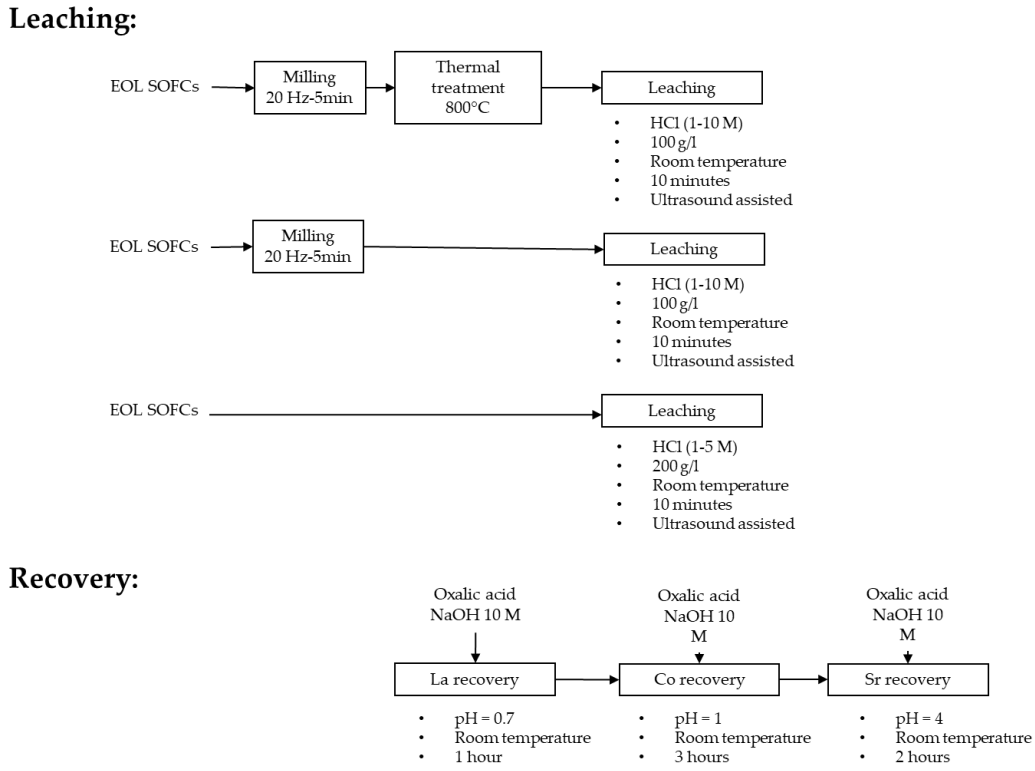

Figure 2. Outline of the experimental tests.

2.3. Recovery of Co, La, and Sr via Chemical Precipitation

Co, La, and Sr were recovered as oxalates from the leachates. Chemical precipitation was achieved in three sequential steps (Figure 2) by adding stoichiometric amounts of oxalic acid (OA) to recover La, Co, and Sr at increasing pH values, according to the literature [29]. Initially, a stoichiometric amount of oxalic acid (OA/La = 2.3) and 10 M NaOH were added until pH 0.7, stirring for 1 h. Then, a stoichiometric amount of oxalic acid (OA/Co = 2) and 10 M NaOH were added until pH 1, stirring for 3 h. Finally, a stoichiometric amount of oxalic acid (OA/Sr = 2) and 10 M NaOH were added until pH 4, stirring for 2 h. Chemical precipitation experiments were conducted on an AREX-6DIGITAL PRO magnetic stirrer using a benchtop pH meter (GEASS PH8+DHS). After precipitation, the solid residues were recovered through a Z206A Hermle Labor Technik centrifuge, rinsed with deionized water, and dried at 60 °C for 10 h in an Argo Lab TCN 30 oven. The recovered products underwent the same characterization described for the ball milled EoL SOC samples. The total recovery efficiency was calculated considering the recovery rate of Co, La, and Sr during the three steps of chemical precipitation compared to the concentration of metals detected in the ball milled EoL SOC samples.

2.4. Preliminary Economic Analysis

A preliminary economic assessment was conducted to compare the explored processes, accounting for the operative costs (EUR) associated with energy and reagents' consumption. The assessment was based on a functional unit equal to 10 g of EoL SOC sample. Energy consumption of the laboratory equipment was directly measured during the experimental activities through a PM10 Maxcio power meter and then normalized considering the maximum processing capacity of each appliance. The prices for energy and reagents were retrieved from Ecoinvent database [30] for reagents (deionized water, hydrochloric acid, oxalic acid, and sodium hydroxide) and from Eurostat [31] for energy for non-household users.

3. Results

3.1. Characterization of SOC Milled Powder (Pre- and Post-Thermal Treatment)

The XRD pattern of the EoL SOC samples after fragmentation and milling (see Appendix A, Figure A1) revealed a mixture of crystalline phases, as expected due to the composite nature of the powders. The observed reflection peaks (Figure A1a) are those typical of the crystalline ZrO_2, metallic Ni (due to the reduction in NiO during cell operation), and perovskite phase. The sample after oxidation at 800 °C confirmed the re-transformation of the Ni metallic phase to NiO and the overall retention of the other crystalline phases.

SEM images (see Appendix A, Figure A2) of the SOCs after ball milling at low (Figure A2a) and high (Figure A2b) magnification showed the efficient comminution of the cells to micronized particles, where a relatively small fraction of aggregates in the range of 20–80 μm were found.

The elemental composition of the SOC sample as revealed by ICP measurements after digestion resulted in 49.2 ± 2%wt. of Ni, 24.7 ± 1.1%wt. of Zr, 3.7 ± 1.6%wt. of Co, 3.5 ± 0.3%wt. of Y, 1.9 ± 0.7%wt. of Sr, 1.0 ± 0.1%wt. of La, 4523 ± 259 ppm of Gd, and 2113 ± 359 ppm of Ce. The elemental composition after thermal pre-treatment was 55 ± 0.7%wt. of Ni (as NiO), 22.1 ± 0.3%wt. of Zr, 4.2 ± 0.1%wt. of Co, 3.1 ± 0.1%wt. of Y, 2.2 ± 0.1%wt. of Sr, 1.1 ± 0.1%wt. of La, 3730 ± 262 ppm of Gd, and 2113 ± 42 ppm of Ce.

3.2. Ultrasound Selective Leaching

The results of the leaching tests performed on the ball milled EoL SOC samples confirmed that HCl is an effective leaching agent for Co, La, and Sr. However, varying leaching parameters and applying a thermal pre-treatment affected both efficiency and selectivity (Figure 3). Ten M HCl without thermal pre-treatment resulted in the highest leaching efficiency for the target metals (98 ± 1% for Co, 96 ± 18% for La, and 99 ± 2% for Sr) but also for Ni (68 ± 1%). These results are consistent with the literature, reporting average HCl leaching efficiency equal to 94% for Co and 97% for La from lithium-ion and nickel metal hydride batteries [29]. Indeed, HCl was reported to be effective in leaching up to 99% of Co from lithium-ion batteries [32], especially during ultrasound-aided leaching [33], and above 90% of Co and La from spent nickel metal hydride batteries [34]. The extremely low leaching efficiency of Y and Zr were justified by the selective behaviour of HCl, which dissolved the perovskite structure of the SOC electrode, leaving unaltered the ceramic YSZ phase of the anode and electrolyte components, as reported by a previous study [28].

However, the high leaching efficiency of HCl for Ni, as reported by the literature [35], compromised the selectivity of the leaching process. Thermal pre-treatment at 800 °C was performed, aiming at Ni oxidation into NiO, as confirmed by XRD spectra (see Appendix A, Figure A1), and achieving 7 ± 1% Ni leaching efficiency (90% decrease compared to the untreated samples). Despite thermal treatment improving the selectivity of leaching by decreasing the solubility of Ni from the NiO phase, it also slightly negatively impacted the leaching efficiency of La (decreased from 96 ± 18% to 92 ± 30%) and Sr (decreased from 99 ± 2% to 94 ± 12%) and more significantly of Co (from 98 ± 1% to 61 ± 2%). The significantly decreased leaching efficiency of Ni after thermal treatment, when present as NiO, can be attributed to a different solubilization mechanism, which significantly affected the dissolution kinetics by HCl at RT [36]. Indeed, the formation of NiO created a passivation layer that hindered the acid dissolution of Ni [37,38] and significantly altered the leaching kinetics, requiring more aggressive conditions, such as higher temperatures or longer leaching times, to dissolve the oxide [39]. The decreased leaching efficiency observed for Co upon thermal treatment suggests modification of the chemical environment for a large fraction of Co sites into the LSC structure. Based on in situ microscopic analyses on

electrode stability when exposed to temperature > 800 °C, this can be tentatively attributed to the pronounced mobility of Co ions along the perovskite structure and their tendency to agglomerate at phase interfaces [40].

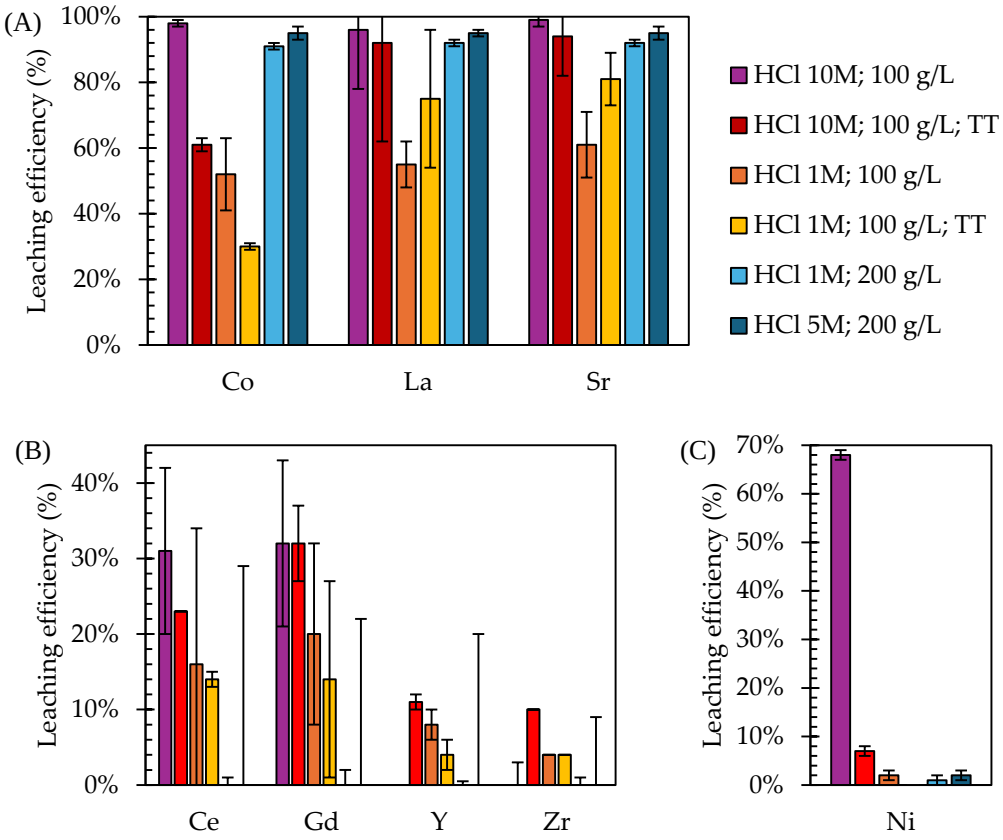

Figure 3. Leaching efficiency achieved on EoL SOC samples for (**A**) target metals from LSC electrode (Co, La, Sr); (**B**) other metals from the barrier layer (Ce, Gd) and from electrolyte/anode electrode (Y, Zr); and (**C**) Ni from the anode electrode (TT: thermal pre-treatment). The tests applying 100 g/L involved ball-milled samples, while 200 g/L regarded direct leaching on cells without any pre-treatment.

Decreasing the HCl concentration from 10 M to 1 M, lower leaching efficiencies were observed for all metals, consistent with a recent study [41] that identified HCl concentration as a key factor influencing the Ni leaching rate, especially at low temperatures and for short leaching times. A total of 52 ± 11% of Co, 55 ± 7% of La, 61 ± 10% of Sr, and 2 ± 1% of Ni were leached with HCl 1 M, while 30 ± 1% of Co, 75 ± 21% of La, 81 ± 8% of Sr, and 0 ± 1% of Ni were leached with HCl 1 M after thermal pre-treatment. Similarly to the results obtained during leaching with 10 M HCl, the effect of thermal treatment diminished the leaching efficiency of Ni (almost 100% decrease compared to the samples without thermal pre-treatment) and Co (42% decrease compared to the samples without thermal pre-treatment). It is worth noticing that decreasing the HCl concentration from 10 M to 1 M without thermal treatment was more effective in limiting Ni leaching (almost 99% reduction) than performing thermal treatment while keeping the HCl concentration at 10 M (90% reduction in Ni leaching efficiency). However, a lower HCl concentration compromised also the leaching efficiency of Co, La, and Sr.

Ultrasound leaching tests were also performed directly on EoL SOC samples, without the manual scratching of the LSC layer, ball milling, and thermal pre-treatment, with HCl 5 and 1 M and applying an S/L equal to 200 g/L. Results were as follows: 91 ± 1% of Co, 92 ± 1% of La, 92 ± 2% of Sr, and 1 ± 1% of Ni were leached with HCl 1 M, and 95 ± 2%

of Co, 95 ± 1% of La, 95 ± 2% of Sr, and 2 ± 1% of Ni were leached with HCl 5 M. The SOC samples showed signs of corrosion (see Appendix A, Figure A3), particularly from 5 M HCl, which, according to the obtained results, led to Ni leaching. Nonetheless, direct leaching tests achieved the highest selectivity of Co, La, and Sr leaching with minimal Ni leaching. Ni leaching efficiency with HCl 5 M directly applied on EoL bulk cells was lower than with HCl 1 M on the milled samples, suggesting that the increase in contact area caused by milling facilitates the exposure of metallic Ni to acidic solution and, thus, its extraction, which greatly hinders the selectivity of the leaching process. Remarkably, increasing the HCl concentration from 1 M to 5 M slightly improved the leaching efficiency of the target metals (4% increase for Co leaching efficiency, 3% for La and Sr); however, it also significantly increased the Ni leaching efficiency. Therefore, the direct leaching applied to the EoL SOC samples allowed a reduction in the HCl concentration.

In conclusion, the performed leaching experiments demonstrated that 10 M HCl without thermal pre-treatment achieved the highest efficiency for Co (98 ± 1%), La (96 ± 18%), and Sr (99 ± 2%) but also caused significant Ni dissolution (68 ± 1%). While thermal pre-treatment effectively reduced Ni dissolution, it had a detrimental effect on the leaching efficiency of the target metals, particularly Co (−42%). Reducing the HCl concentration and increasing the S/L ratio in the direct leaching tests improved selectivity, also avoiding thermal treatment and milling. This approach reduced Ni leaching by almost 100% while still achieving the efficient recovery of the target metals, e.g., up to 95% for Co, La, and Sr with 5 M HCl and 91% for Co, La, and Sr using 1 M HCl. The residues remaining after the ultrasound HCl leaching tests applied to the EoL SOC samples can be involved in further processes aimed at the recovery of Ni and YSZ.

3.3. Recovery via Chemical Precipitation

After leaching, three chemical precipitation steps at pH 0.7, 1, and 4 were carried out to recover Co, La, and Sr oxalates, which, upon calcination, are easily converted into the metal oxides used for manufacturing the LSC electrodes of novel SOCs. The recovery efficiencies achieved for Co, La, and Sr (Figure 4) were strongly influenced by the different leaching efficiencies discussed in Section 3.2 and the efficiency of recovery itself. Specifically, the increase in the HCl concentration during leaching enabled the dissolution of greater amounts of Co, La, and Sr, which could then be recovered through precipitation. However, a higher HCl concentration during leaching also increased the H_3O^+ concentration in the solution, which made the pH control during the precipitation more challenging and consequently hindered both the recovery efficiency and purity of precipitates.

The recovery efficiency was calculated for La, Co, and Sr (based on their concentrations detected in the SOC samples) after leaching in HCl followed by recovery via chemical precipitation. The recovery efficiencies after leaching with 10 M HCl were 85 ± 20% for Co, 82 ± 24% for La, and 15 ± 4% for Sr from milled samples without thermal pre-treatment, while 47 ± 3% of Co, 69 ± 15% of La, and 52 ± 20% of Sr were recovered after thermal pre-treatment. Lower recovery efficiencies were found after leaching with 1 M HCl: 46 ± 16% of Co, 18 ± 7% of La, and 35 ± 14% of Sr were recovered without thermal pre-treatment, while 2 ± 3% of Co, 49 ± 3% of La, and 55 ± 18% of Sr were recovered from thermally pre-treated samples. The recovery efficiencies obtained after direct leaching tests were 42 ± 5% for Co, 93 ± 6% for La, and 33 ± 9% for Sr after leaching with 1 M HCl and 47 ± 7% for Co, 76 ± 10% for La, and 62 ± 8% for Sr after leaching with 5 M HCl. The mentioned challenges in pH control during chemical precipitation occurred; applying more concentrated leaching solutions was confirmed by the higher standard deviations observed in the recovery efficiency values.

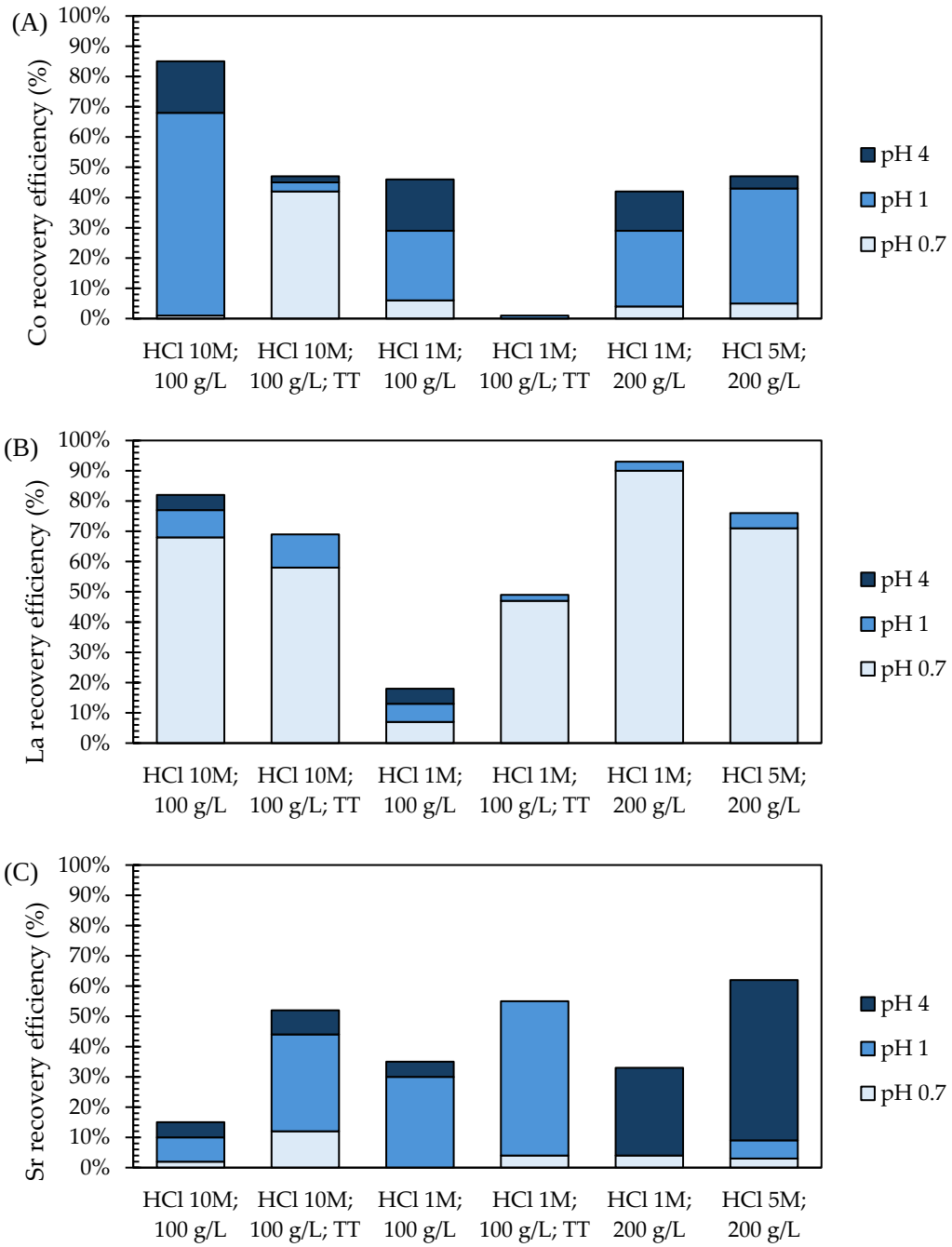

Figure 4. Recovery efficiencies achieved for (**A**) Co, (**B**) La, and (**C**) Sr in the sequential precipitation steps from milled EoL SOC samples.

Based on the results in Figure 4 and the characterization of the recovered precipitates (see Appendix A, Figures A4–A9), chemical precipitation did not allow a selective recovery of distinct Co, La, and Sr oxalates. However, a trend can be observed, since lanthanum oxalates were identified at pH 0.7, lanthanum and cobalt oxalates at pH 1, and strontium oxalates at pH 4. Chemical precipitation at pH 1 was less efficient and selective than at pH 0.7, particularly increasing the HCl concentration during leaching. Specifically, in the precipitates obtained at pH 1 from 5 M HCl leaching, which dissolved 2 ± 1% of Ni, also nickel oxalate was identified. The coprecipitation of Co-Ni oxalates was due to the competing behaviour of Co and Ni during precipitation [42]. Biphasic precipitates may find various industrial applications, e.g., La-Co oxalates could be used in the manufacture of SOC cathodes [43], while Co-Ni oxalates might be used in the production of lithium-ion

batteries [44]. However, the presence of La, Co, and Ni in the same precipitate poses a challenge for potential applications.

Conversely, purification of the recovered fraction may be achievable through solvent extraction [45]. Specifically, Cyanex 272 can be used to separate Co and Ni from acid solutions and recover $CoSO_4 \cdot H_2O$ with 99.9% purity [46]. However, it is important to note that La also exhibits a significant affinity for Cyanex 272 [47]. Therefore, a tailored solvent extraction approach for the recycling of Co, La, and Sr from end-of-life SOCs should be further developed.

While the results obtained in this study show promising outcomes, the efficiency of metal recovery, particularly during the precipitation phase, could be further enhanced by optimizing operational conditions, such as pH, temperature, and the molar ratio of precipitation agents for each target metal [48]. Additionally, combining leaching with advanced techniques, such as solvent extraction [46,47] or electrochemical methods [49] for metal separation during precipitation, offers promising strategies by ensuring precise control over the recovery of specific metals. In conclusion, recovery exhibited different efficiency towards La, Co, and Sr depending on the leaching conditions applied. The highest La recovery was achieved with HCl 200 g/L 1 M (93%), 5 M (76%), and 100 g/L 10 M (82%). The greatest Co recovery was obtained with HCl 100 g/L 10 M (85%), while other leaching conditions limited recovery to 45–47%. Sr recovery was higher (62%) after leaching with 200 g/L HCl 5 M, while 200 g/L HCl 1 M achieved 33% and other leaching conditions obtained recovery in the range of 15–55%.

3.4. Preliminary Economic Assessment

The preliminary economic assessment, based on the operative costs (energy and reagents) associated with recycling 10 g of EoL SOC samples and comparing the different processes applied, was broken down into three major steps: pre-treatment (milling and eventually thermal treatment), leaching, and recovery via chemical precipitation (including centrifugation). The results ranged between EUR 0.05 and EUR 1.47, and energy demand was the main contributor (Figure 5). Specifically, when thermal pre-treatment was applied, the operative costs were EUR 1.47 for leaching with 10 M HCl and EUR 1.46 for leaching with 1 M HCl. In contrast, without thermal pre-treatment, the operative costs were cut by 38% and were EUR 0.91 and EUR 0.90, respectively. Also, milling represented a significant cost driver; while this can be ascribed to the small scale of the laboratory milling equipment and scaling up, the process could significantly reduce the associated energy demand. This preliminary economic assessment was based on a functional unit of 10 g of EoL SOC samples, corresponding to the amount of material effectively treated in the experimental activities of this study. However, it is important to note that scaling up the process, particularly the milling stage, could significantly reduce energy demand, as industrial-scale milling equipment tends to be more energy efficient than laboratory-scale equipment. Similarly, although thermal pre-treatment resulted in higher operational costs, optimizing thermal treatment conditions and implementing continuous processes could further reduce energy consumption and lower operational costs in larger-scale operations. The lowest operative costs are represented by direct leaching without milling and thermal treatment and were equal to EUR 0.05 with 1 M HCl and EUR 0.06 with 5 M HCl.

Thus, avoiding pre-treatments, reducing the HCl concentration, and increasing the solid-to-liquid ratio appear to be the optimal strategy for the selective recycling of LSC from EoL SOCs. Decreasing the HCl concentration is significant from economic and environmental points of view. Indeed, decreasing HCl concentrations leads to lower reagent consumption for neutralizing the solution pH during precipitation and reduced operational costs of the process. Moreover, the use of HCl during hydrometallurgical recycling should

be limited as it can result in the emission of toxic chlorine gas [50]. Additionally, alternative leaching agents could offer a viable solution to reduce the environmental impact of the recycling processes. For instance, organic acids or more environmentally friendly chelating agents might offer the selective recovery of target metals while reducing the environmental footprint [51,52]. Moreover, optimizing the leaching parameters such as temperature, leaching time, and stirring conditions could potentially increase the dissolution rate of the target metals without compromising selectivity. Studies showed that mild temperature elevations and extended leaching times may enhance the leaching efficiency of metals like Co, La, and Sr, and it is possible that such conditions could be adapted to the specific needs of LSC recycling [29].

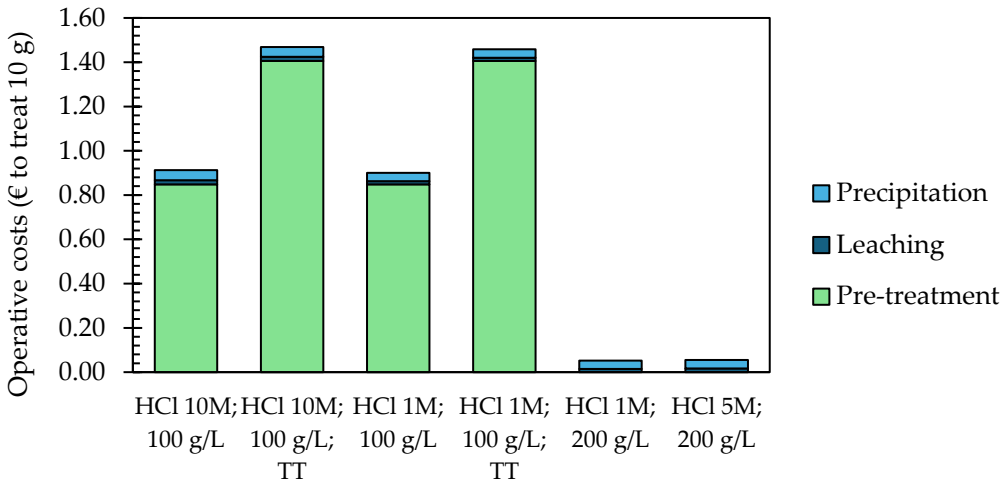

Figure 5. Operative costs required to recycle 10 g of EoL SOC sample by applying different leaching conditions (TT: thermal pre-treatment).

In conclusion, the optimal selective recycling strategy for SOCs' samples, which reduces costs by up to 96% (from EUR 1.47 to EUR 0.05) and minimizes the environmental impact, involves avoiding energy-intensive pre-treatments and lowering reagent consumption.

4. Conclusions

This study presents a selective ultrasound leaching process based on HCl to recycle Co, La, and Sr from EoL SOCs, comparing different strategies to increase leaching and recovery efficiency and selectivity and assessing the economic viability. The main results of the leaching tests are as follows:

- Leaching tests on ball-milled SOC samples with 10 M HCl and a 100 g/L solid-to-liquid (S/L) ratio achieved the highest efficiencies for Co (98%), La (96%), and Sr (99%) but also for Ni (68%), limiting selectivity.
- The thermal pre-treatment of milled powders re-oxidized metallic Ni into NiO, increasing selectivity by reducing Ni leaching by 90%. However, this also resulted in a reduction in Co leaching efficiency by 42% and La and Sr by 9%.
- Leaching tests with a lower concentration of 1 M HCl reduced Ni leaching by 97% in the milled SOC samples without thermal pre-treatment but also decreased the leaching of target metals by up to 60%. For SOC samples oxidized by thermal pre-treatment, Ni leaching was completely avoided during 1 M HCl leaching, while the leaching efficiencies for La, Co, and Sr were 75%, 30%, and 81%, respectively.

- The direct leaching of EoL SOCs (not subjected to any milling and thermal treatment) employing 200 g/L of HCl obtained minimal Ni leaching and 95% of Co, La, and Sr when 5 M HCl was applied and 91–92% of Co, La, and Sr with 1 M HCl.

Chemical precipitation recovered Co, La, and Sr as mixed oxalates, with efficiency and selectivity affected by leaching conditions. Ten M HCl dosed at 100 g/L on ball-milled samples provided the greatest La (82%) and Co (85%) recovery efficiency but introduced challenges in pH control during precipitation, resulting in lower purity of the recovered precipitates and low recovery for Sr (15%). Direct leaching with 200 g/L of 1 M HCl followed by chemical precipitation produced oxalates of higher purity with a recovery efficiency of 42% for Co, 93% for La, and 33% for Sr, while 5 M HCl led to recovery efficiencies equal to 47% for Co, 76% for La, and 62% for Sr. A preliminary economic assessment revealed that the operational costs of the investigated processes ranged between EUR 0.05 and EUR 1.47 per 10 g of EoL SOC sample, with the lowest value corresponding to direct leaching in 200 g/L 1 M HCl and the highest to 10 M HCl leaching of ball-milled samples after thermal pre-treatment. Direct leaching in 200 g/L 1 M HCl followed by chemical precipitation offered the best trade-off, also considering the purity of recovered oxalates, reducing the costs by up to 96% compared to the most expensive option involving thermal treatment and 100 g/L 10 M HCl. Direct leaching not only lowered operational costs but also minimized environmental impacts by reducing reagent consumption and energy use.

In conclusion, this study investigated EoL SOC recycling at lab scale, with specific interest for the recovery of La, Co, and Sr from the LSC layer, overlooked by the existing literature. Scaling up these processes could potentially alter cost dynamics, and more research is needed to evaluate their feasibility and cost effectiveness. Further research should address the optimization of leaching and precipitation conditions, including alternative, more environmentally friendly reagents, such as leaching based on mild organic acids.

Author Contributions: Conceptualization, S.F. (Sonia Fiorilli) and S.F. (Silvia Fiore); methodology, M.B. and S.F. (Silvia Fiore); investigation, M.B. and S.S.; data curation, M.B. and S.S.; writing—original draft preparation, M.B.; writing—review and editing, F.S., S.F. (Sonia Fiorilli), and S.F. (Silvia Fiore); visualization, M.B. and S.S.; supervision, S.F. (Silvia Fiore).; funding acquisition, F.S., S.F. (Sonia Fiorilli), and S.F. (Silvia Fiore). All authors have read and agreed to the published version of the manuscript.

Funding: The research was performed within the BEST4Hy Horizon 2020 project, which has received funding from the Fuel Cells and Hydrogen 2 Joint Undertaking (now Clean Hydrogen Partnership) under Grant Agreement No. 101007216. This Joint Undertaking receives support from the European Union's Horizon 2020 Research and Innovation program, Hydrogen Europe, and Hydrogen Europe Research.

Data Availability Statement: Data are contained within the article.

Conflicts of Interest: The authors declare no conflicts of interest.

Abbreviations

The following abbreviations are used in this manuscript:

EoL	End of life
GHGs	Greenhouse gasses
LSC	Strontium-doped lanthanum-cobalt oxides
SOCs	Solid oxide cells
YSZ	Yttria-stabilized Zirconia

Appendix A

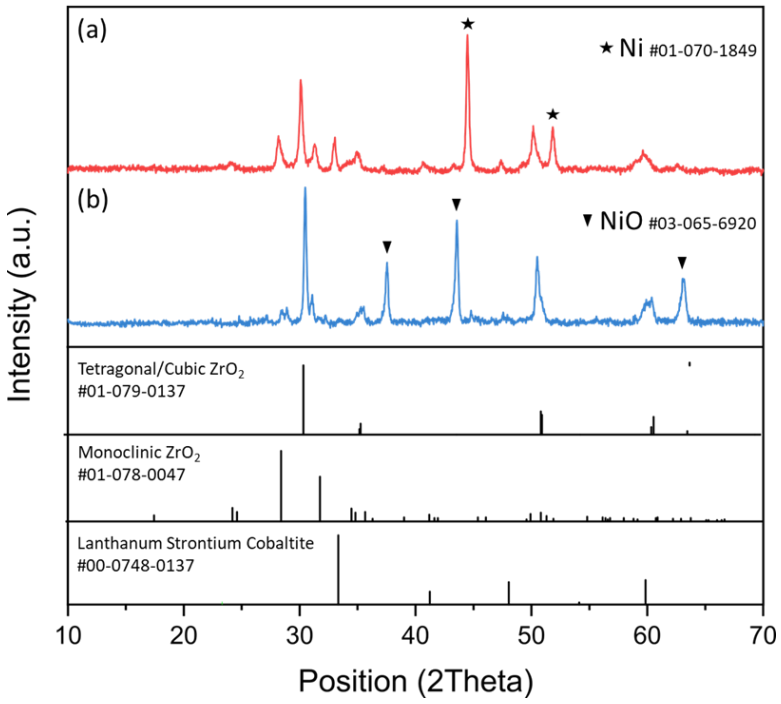

Figure A1. XRD spectra of (**a**) milled EoL SOC sample and (**b**) milled SOC sample after oxidation at 800 °C for 3 h. The diffraction patterns of the expected crystalline phases and related reference codes are reported for comparison.

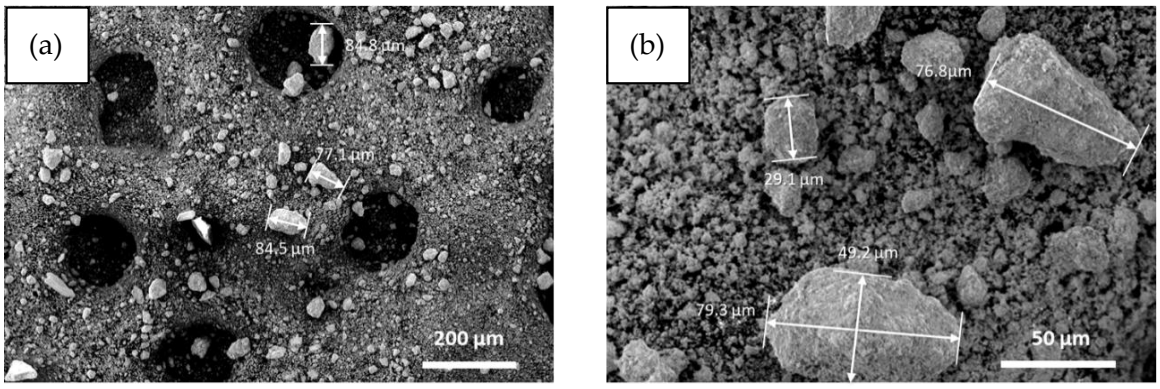

Figure A2. SEM images of EoL SOC after milling at low (**a**) and high magnification (**b**).

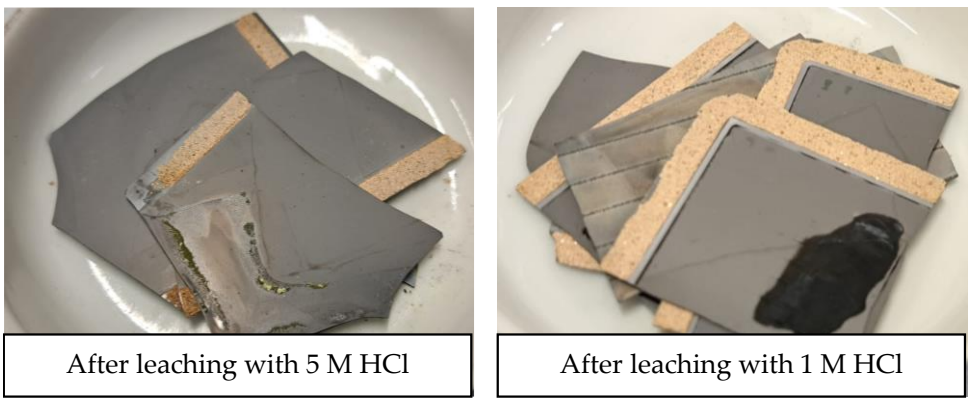

Figure A3. EoL SOC samples after direct leaching in HCl at room temperature for 10 min applying a 200 g/L solid-to-liquid ratio.

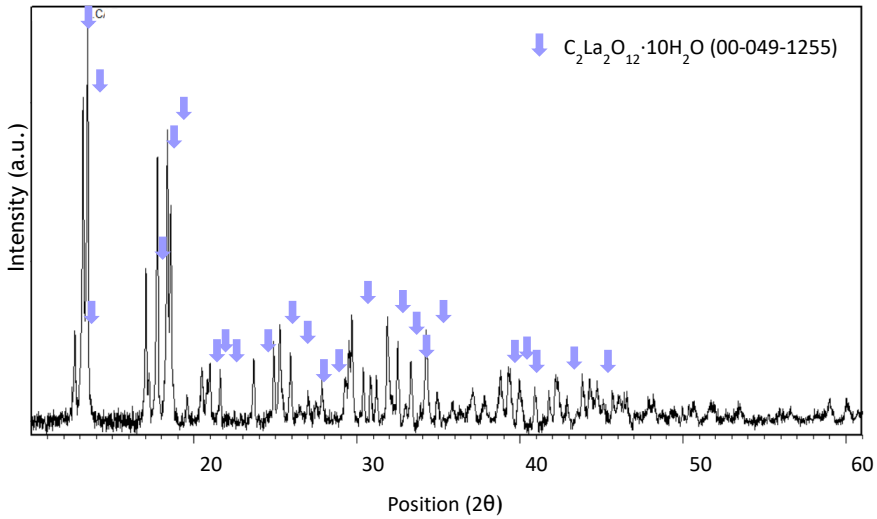

Figure A4. XRD spectrum of precipitate obtained at pH 0.7 after leaching with HCl 1 M, an S/L ratio of 200 g/L for 10 min at room temperature.

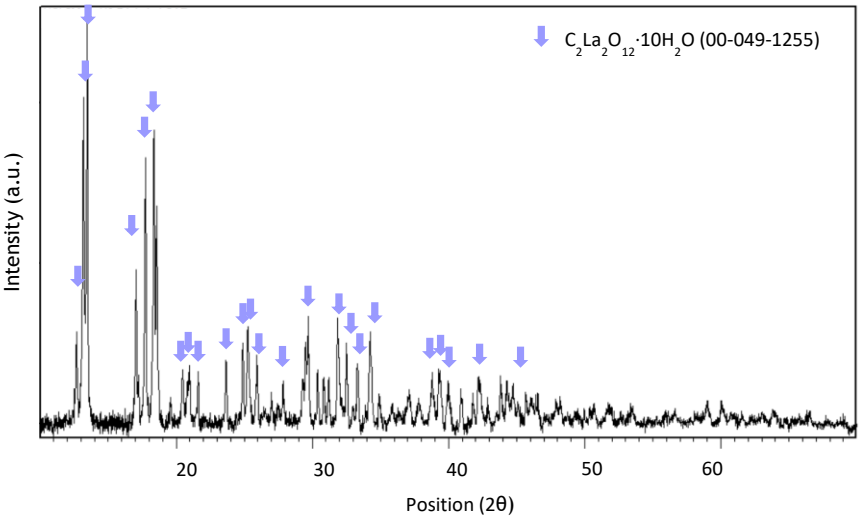

Figure A5. XRD spectrum of precipitate obtained at pH 0.7 after leaching with HCl 5 M, an S/L ratio of 200 g/L for 10 min at room temperature.

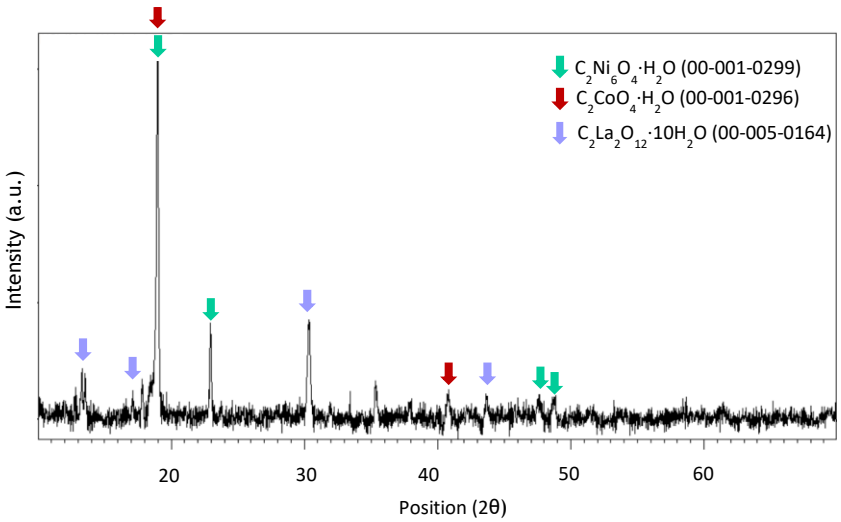

Figure A6. XRD spectrum of precipitate obtained at pH 1 after leaching with HCl 1 M, an S/L ratio of 200 g/L for 10 min at room temperature.

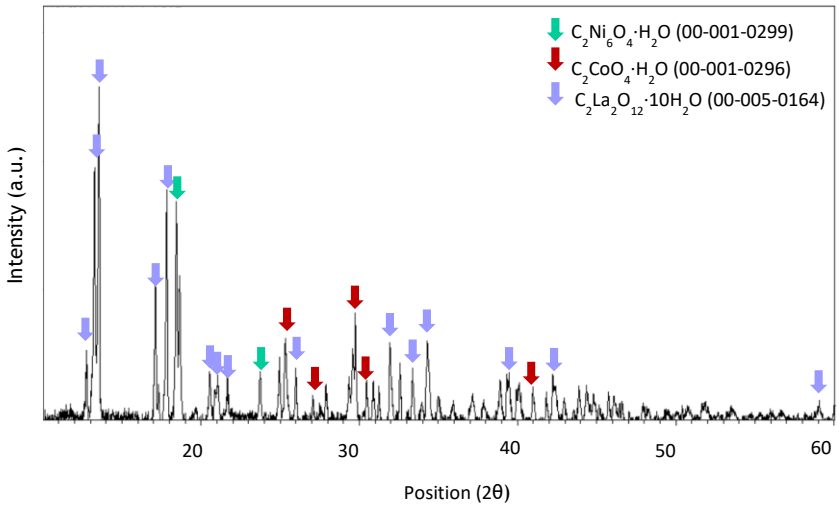

Figure A7. XRD spectrum of precipitate obtained at pH 1 after leaching with HCl 5 M, an S/L ratio of 200 g/L for 10 min at room temperature.

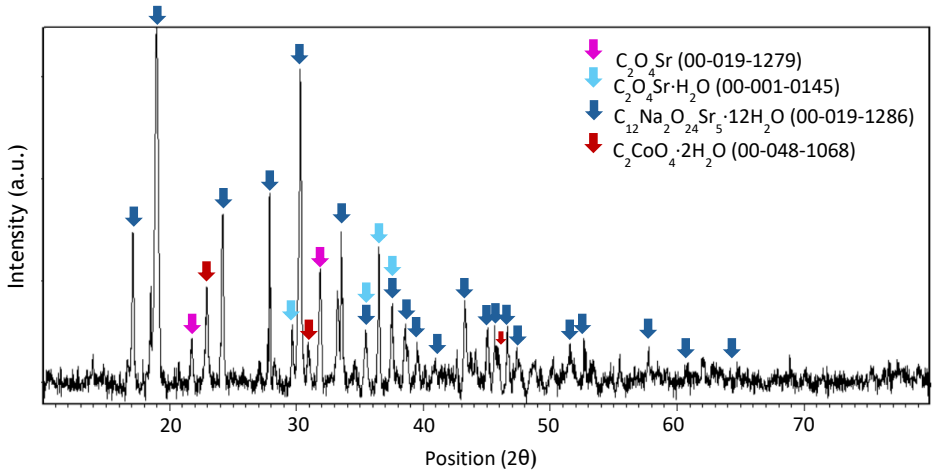

Figure A8. XRD spectrum of precipitate obtained at pH 4 after leaching with HCl 1 M, an S/L ratio of 200 g/L for 10 min at room temperature.

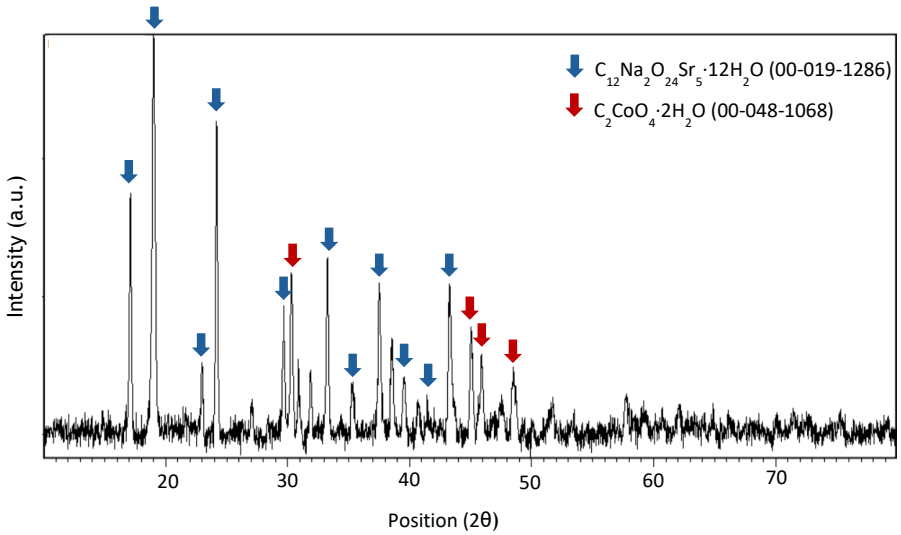

Figure A9. XRD spectrum of precipitate obtained at pH 4 after leaching with HCl 5 M, an S/L ratio of 200 g/L for 10 min at room temperature.

References

1. Subotić, V.; Napporn, T.W. Nanostructured Metal Oxides for High-Performance Solid Oxide Fuel Cells (SOFCs). In *Metal Oxide-Based Nanostructured Electrocatalysts for Fuel Cells, Electrolyzers, and Metal-Air Batteries*; Elsevier: Amsterdam, The Netherlands, 2021; pp. 235–261.
2. Tsai, S.-Y.; Fung, K.-Z. Progress and Prospects of Intermsediate-Temperature Solid Oxide Fuel Cells. In *Energy Storage and Conversion Materials: Properties, Methods, and Applications*; CRC Press: Boca Raton, FL, USA, 2023; pp. 265–276. [CrossRef]
3. Smith, L.; Ibn-Mohammed, T.; Yang, F.; Reaney, I.M.; Sinclair, D.C.; Koh, S.C.L. Comparative Environmental Profile Assessments of Commercial and Novel Material Structures for Solid Oxide Fuel Cells. *Appl. Energy* **2019**, *235*, 1300–1313. [CrossRef]
4. Shen, Y.; Yang, Y.; Song, L.; Lei, T. Environmental Impact Assessment of Solid Oxide Fuel Cell Power Generation System Based on Life Cycle Assessment—A Case Study in China. *Sustainability* **2024**, *16*, 3863. [CrossRef]
5. Du, Y.; Cheekatamarla, P. SOFC's Bumpy Road and Hopeful Future-A Case Study. In Proceedings of the ECS Transactions, Kyoto, Japan, 8–13 September 2019; Volume 91, pp. 179–186.
6. Yatoo, M.A.; Habib, F.; Malik, A.H.; Qazi, M.J.; Ahmad, S.; Ganayee, M.A.; Ahmad, Z. Solid-Oxide Fuel Cells: A Critical Review of Materials for Cell Components. *MRS Commun.* **2023**, *13*, 378–384. [CrossRef]
7. Gil-Muñoz, G.; Alcañiz-Monge, J. Examining the Effect of Zirconium Doping in Lanthanum Nickelate Perovskites on Their Performance as Catalysts for Dry Methane Reforming. *J. Environ. Chem. Eng.* **2025**, *13*, 115387. [CrossRef]
8. Han, M.; Zhang, Y. Ceramic Materials for Solid Oxide Fuel Cell. *Kuei Suan Jen Hsueh Pao/J. Chin. Ceram. Soc.* **2017**, *45*, 1548–1554. [CrossRef]
9. Wang, Y.; Song, M. Redox Stability Optimization in Anode-Supported Solid Oxide Fuel Cells. *Materials* **2024**, *17*, 3257. [CrossRef]
10. Xu, H.; Zhao, N.; Zhang, H.; Xue, Q.; Zhang, J.; Huang, X. Research Progress in Zirconium-Based Electrolyte Applied in Solid Oxide Fuel Cell. *Xiyou Jinshu/Chin. J. Rare Met.* **2017**, *41*, 437–444. [CrossRef]
11. Predoana, L.; Malič, B.; Petrescu, S.; Preda, S.; Zaharescu, M. Influence of the Precursors on the La0.5Sr0.5CoO3 Formation by Water-Based Sol-Gel Method. *Rev. Roum. Chim.* **2018**, *63*, 711–718.
12. Qiang, J.; Wang, D.; Hui, S. Synthesis of La1-XSrxCoO3-Δand Its REDOX Performance in Air. *J. Environ. Chem. Eng.* **2022**, *10*, 108794. [CrossRef]
13. European Commission. *Communication from the Commission to the European Parliament, the Council, the European Economic and Social Committee and the Committee of the Regions-Critical Raw Materials Resilience: Charting a Path towards Greater Security and Sustainability*; European Commission: Brussels, Belgium, 2020.
14. Campos-Carriedo, F.; Iribarren, D.; Calvo-Rodríguez, F.; García-Díaz, Á.; Dufour, J. Methodological and Practical Lessons Learned from Exploring the Material Criticality of Two Hydrogen-Related Products. *Resour. Conserv. Recycl.* **2024**, *206*, 107614. [CrossRef]
15. Mishra, S.; Panda, S.; Akcil, A. Environmental and Social Impacts of Recycling Critical Raw Materials. In *Critical Materials and Sustainability Transition*; CRC Press: Boca Raton, FL, USA, 2023; pp. 86–101.
16. Sultana, I.; Chen, Y.; Huang, S.; Rahman, M.M. Recycled Value-Added Circular Energy Materials for New Battery Application: Recycling Strategies, Challenges, and Sustainability-a Comprehensive Review. *J. Environ. Chem. Eng.* **2022**, *10*, 108728. [CrossRef]
17. Valente, A.; Iribarren, D.; Dufour, J. End of Life of Fuel Cells and Hydrogen Products: From Technologies to Strategies. *Int. J. Hydrogen Energy* **2019**, *44*, 20965–20977. [CrossRef]
18. Sarner, S.; Schreiber, A.; Menzler, N.H.; Guillon, O.; Sarner, S.; Menzler, N.H.; Guillon, O.; Schreiber, A. Recycling Strategies for Solid Oxide Cells. *Adv. Energy Mater.* **2022**, *12*, 2201805. [CrossRef]
19. Dragan, M. Closing the Loop: Solid Oxide Fuel and Electrolysis Cells Materials for a Net-Zero Economy. *Materials* **2024**, *17*, 6113. [CrossRef]
20. Sarner, S.; Menzler, N.H.; Malzbender, J.; Hilger, M.; Sebold, D.; Weber, A.; Guillon, O. Towards a Scalable Recycling Process for Ceramics in Fuel-Electrode-Supported Solid Oxide Cells. *Green Chem.* **2025**, *27*, 2252–2262. [CrossRef]
21. Saffirio, S.; Pylypko, S.; Fiorot, S.; Schiavi, I.; Fiore, S.; Santarelli, M.; Ferrero, D.; Smeacetto, F.; Fiorilli, S. Hydrothermally-Assisted Recovery of Yttria- Stabilized Zirconia (YSZ) from End-of-Life Solid Oxide Cells. *Sustain. Mater. Technol.* **2022**, *33*, e00473. [CrossRef]
22. Yenesew, G.T.; Quarez, E.; Salle, A.L.G.L.; Nicollet, C.; Joubert, O. Recycling and Characterization of End-of-Life Solid Oxide Fuel/Electrolyzer Ceramic Material Cell Components. *Resour. Conserv. Recycl.* **2023**, *190*, 106809. [CrossRef]
23. Kaiser, C.; Buchwald, T.; Peuker, U.A. Ultrasonic Decoating as a New Recycling Path to Separate Oxygen Side Layers of Solid Oxide Cells. *Green Chem.* **2023**, *26*, 960–967. [CrossRef]
24. Mori, M.; Gramc, J.; Hojkar, D.; Lotrič, A.; Smeacetto, F.; Fiorilli, S.; Fiore, S.; Stropnik, R. New Life Cycle Inventories for End-of-Life Solid Oxide Cells Based on Novel Recycling Processes for Critical Solid Oxide Cell Materials. *Int. J. Hydrogen Energy* **2024**, *104*, 635–650. [CrossRef]
25. Saffirio, S.; Anelli, S.; Pylypko, S.; Rath, M.K.; Smeacetto, F.; Fiorilli, S. Recycling and Reuse of Ceramic Materials from Components of Waste Solid Oxide Cells (SOCs). *Ceram. Int.* **2024**, *50*, 34472–34477. [CrossRef]

26. Sutama, D.K.; Prasetya, A.; Petrus, H.T.B.M.; Astuti, W. Recovery of Cobalt and Molybdenum from Consumed Catalyst Using Hydrochloric Acid. In Proceedings of the IOP Conference Series: Earth and Environmental Science, Banda Aceh, Indonesia, 21 September 2021; Volume 882.
27. Peeters, N.; Binnemans, K.; Riaño, S. Recovery of Cobalt from Lithium-Ion Battery Cathode Material by Combining Solvoleaching and Solvent Extraction. *Green Chem.* **2022**, *24*, 2839–2852. [CrossRef]
28. Mitterdorfer, A.; Gauckler, L.J. La2Zr2O7 Formation and Oxygen Reduction Kinetics of the La0.85Sr0.15MnyO3, O2(g) | YSZ System. *Solid State Ion.* **1998**, *111*, 185–218. [CrossRef]
29. Mas, A.B.; Fiore, S.; Fiorilli, S.; Smeacetto, F.; Santarelli, M.; Schiavi, I. Analysis of Lanthanum and Cobalt Leaching Aimed at Effective Recycling Strategies of Solid Oxide Cells. *Sustainability* **2022**, *14*, 3335. [CrossRef]
30. Ecoinvent Ecoinvent v3.8-Ecoinvent. Available online: https://ecoinvent.org/the-ecoinvent-database/data-releases/ecoinvent-3-8/ (accessed on 8 March 2023).
31. Eurostat Electricity Prices for Non-Household Consumers-Bi-Annual Data (from 2007 Onwards). Available online: https://ec.europa.eu/eurostat/databrowser/view/nrg_pc_205/default/table?lang=en&category=nrg.nrg_price.nrg_pc (accessed on 29 July 2024).
32. Wang, R.C.; Lin, Y.C.; Wu, S.H. A Novel Recovery Process of Metal Values from the Cathode Active Materials of the Lithium-Ion Secondary Batteries. *Hydrometallurgy* **2009**, *99*, 194–201. [CrossRef]
33. Guzolu, J.S.; Gharabaghi, M.; Mobin, M.; Alilo, H. Extraction of Li and Co from Li-Ion Batteries by Chemical Methods. *J. Inst. Eng. Ser. D* **2017**, *98*, 43–48. [CrossRef]
34. Lie, J.; Lin, Y.C.; Liu, J.C. Process Intensification for Valuable Metals Leaching from Spent NiMH Batteries. *Chem. Eng. Process.-Process Intensif.* **2021**, *167*, 108507. [CrossRef]
35. Tang, Y.C.; Wang, J.Z.; Chou, C.M.; Shen, Y.H. Material and Waste Flow Analysis for Environmental and Economic Impact Assessment of Inorganic Acid Leaching Routes for Spent Lithium Batteries' Cathode Scraps. *Batteries* **2023**, *9*, 207. [CrossRef]
36. Pichugina, N.M.; Kutepov, A.M.; Gorichev, I.G.; Izotov, A.D.; Zaitsev, B.E. Dissolution Kinetics of Nickel(II) and Nickel(III) Oxides in Acid Media. *Transl. Teor. Osn. Khimicheskoi Tekhnologii* **2002**, *36*, 533–543.
37. Wang, Y.; Chang, X.; Chen, M.; Qin, W.; Han, J. Effective Extraction of Nickel and Cobalt from Sintered Nickel Alloy via Reduction Roasting and Leaching. *Miner. Eng.* **2023**, *203*, 108336. [CrossRef]
38. Mir, S.; Shukla, N.; Dhawan, N. Investigation of Microwave and Thermal Processing of Electrode Material of End-of-Life Ni-MH Battery. *JOM* **2021**, *73*, 951–961. [CrossRef]
39. Wang, Y.W.; Qin, W.Q.; Han, J.W. Efficient Nickel Extraction from Nickel Matte by Combined Atmospheric-Oxygen Pressure Acid Leaching: Thermodynamic Analysis and Sulfur Conversion Mechanism. *Miner. Eng.* **2024**, *207*, 108577. [CrossRef]
40. Gualandris, F.; Simonsen, S.B.; Wagner, J.B.; Sanna, S.; Muto, S.; Kuhn, L.T. In Situ TEM Analysis of a Symmetric Solid Oxide Cell in Oxygen and Vacuum–Cation Diffusion Observations. *ECS Trans.* **2017**, *75*, 123–133. [CrossRef]
41. Balázs Illés, I.; Kékesi, T. Extraction of Pure Co, Ni, Mn, and Fe Compounds from Spent Li-Ion Batteries by Reductive Leaching and Combined Oxidative Precipitation in Chloride Media. *Miner. Eng.* **2023**, *201*, 108169. [CrossRef]
42. Gerold, E.; Luidold, S.; Antrekowitsch, H. Selective Precipitation of Metal Oxalates from Lithium Ion Battery Leach Solutions. *Metals* **2020**, *10*, 1435. [CrossRef]
43. Chen, Y.; Cai, Z.; Kuru, Y.; Ma, W.; Tuller, H.L.; Yildiz, B. Electronic Activation of Cathode Superlattices at Elevated Temperatures-Source of Markedly Accelerated Oxygen Reduction Kinetics. *Adv. Energy Mater.* **2013**, *3*, 1221–1229. [CrossRef]
44. Zhao, T.; Ji, R.; Meng, Y. The Role of Precipitant in the Preparation of Lithium-Rich Manganese-Based Cathode Materials. *Chem. Phys. Lett.* **2019**, *730*, 354–360. [CrossRef]
45. Ajiboye, A.E.; Dzwiniel, T.L. Sequential Recovery of Critical Metals from Leached Liquor of Processed Spent Lithium-Ion Batteries. *Batteries* **2023**, *9*, 549. [CrossRef]
46. Meshram, P.; Virolainen, S.; Abhilash; Sainio, T. Solvent Extraction for Separation of 99.9% Pure Cobalt and Recovery of Li, Ni, Fe, Cu, Al from Spent LIBs. *Metals* **2022**, *12*, 1056. [CrossRef]
47. Banda, R.; Jeon, H.S.; Lee, M.S. Solvent Extraction Separation of La from Chloride Solution Containing Pr and Nd with Cyanex 272. *Hydrometallurgy* **2012**, *121–124*, 74–80. [CrossRef]
48. Free, M.L. *Hydrometallurgy*; Springer Nature: Dordrecht, The Netherlands, 2022. [CrossRef]
49. Shahid, M.; Ashoka Sahadevan, S.; Ramani, V.; Sankarasubramanian, S. Recommended Practices for the Electrochemical Recovery of Cobalt from Lithium Cobalt Oxide: A Case Study of the Choline Chloride: Ethylene Glycol Deep Eutectic Solvent. *ChemSusChem* **2024**, *18*, e202401205. [CrossRef]
50. Peeters, N.; Binnemans, K.; Riaño, S. Solvometallurgical Recovery of Cobalt from Lithium-Ion Battery Cathode Materials Using Deep-Eutectic Solvents. *Green Chem.* **2020**, *22*, 4210–4221. [CrossRef]

51. Musariri, B.; Akdogan, G.; Dorfling, C.; Bradshaw, S. Evaluating Organic Acids as Alternative Leaching Reagents for Metal Recovery from Lithium Ion Batteries. *Miner. Eng.* **2019**, *137*, 108–117. [CrossRef]
52. Gerold, E.; Schinnerl, C.; Antrekowitsch, H. Critical Evaluation of the Potential of Organic Acids for the Environmentally Friendly Recycling of Spent Lithium-Ion Batteries. *Recycling* **2022**, *7*, 4. [CrossRef]